ENVIRONMENTAL RESEARCH
LETTERS

LETTER • OPEN ACCESS

Comparing process-based models with the inventory approach to predict CH_4 emission of livestock enteric fermentation

To cite this article: Jianan Zhang *et al* 2023 *Environ. Res. Lett.* **18** 035002

ENVIRONMENTAL RESEARCH
LETTERS

LETTER

Comparing process-based models with the inventory approach to predict CH_4 emission of livestock enteric fermentation

Jianan Zhang[1], **Lan Chen**[2], **Yizhao Chen**[1,*] and **Pavel Groisman**[3,4]

[1] Joint Innovation Center for Modern Forestry Studies, College of Biology and the Environment, Nanjing Forestry University, Nanjing, Jiangsu, People's Republic of China
[2] College of Agricultural and Biotechnology, Zhejiang University, Hangzhou, People's Republic of China
[3] Hydrology Science and Services Corp., Asheville, NC, United States of America
[4] North Carolina State University at NOAA National Centers for Environment Information, Asheville, NC, United States of America
[*] Author to whom any correspondence should be addressed.

E-mail: chenyzvest@gmail.com

Keywords: livestock, CH_4, emission factors, process-based models, inventory-based models, enteric fermentation, Inner Mongolia

Supplementary material for this article is available online

OPEN ACCESS

RECEIVED
14 June 2022

REVISED
23 January 2023

ACCEPTED FOR PUBLICATION
27 January 2023

PUBLISHED
17 February 2023

Abstract

Livestock production is the largest anthropogenic methane (CH_4) source globally over the decades. Enteric fermentation of ruminants is responsible for the majority of global livestock CH_4 emissions. Both inventory-based models (IvtMs) and process-based models (PcMs) are extensively used to assess the livestock CH_4 emission dynamics. However, the model performance and the associated uncertainty have not been well quantified and understood, which greatly hamper our credibility of the regional and global CH_4 emission predictions. In this study, we compared the CH_4 emissions of livestock enteric fermentation ($CH_{4,ef}$) predicted by multiple IvtMs and PcMs across Inner Mongolia, a region dominated by typical temperate grasslands that are widely used for animal husbandry. Twenty predictions from five IvtMs, and ten predations from five PcMs were explicitly calculated and compared for the reference year of 2006. The $CH_{4,ef}$ predicted from PcMs is lower than IvtMs and the variation between PcMs is substantially higher, i.e. 0.34 ± 0.36 g CH_4/m^2 yr and 0.78 ± 0.14 g CH_4/m^2 yr for PcMs and IvtMs, respectively. Different model strategies undertaken, i.e. the demand-oriented strategy for IvtMs and the resource-demand co-determined one for PcMs, cause the different predictions of $CH_{4,ef}$ between the two model groups. Using the results from IvtMs as the baseline scalar, we identified and benchmarked the performance of individual PcMs in the study region. The quantitative information provided can facilitate the understanding of key principles and processes of $CH_{4,ef}$ estimations, which will contribute to the future model development of global CH_4 emission.

1. Introduction

Methane (CH_4) is one of the most important greenhouse gases (GHGs) globally. According to the fifth report of the United Nations Framework Convention on Climate Change (IPCC 2013), its global warming potential is 100 year time horizon value of 28 and accounts for approximately 18% of the total direct warming effect caused by GHG (Montzka *et al* 2011). Therefore, a proper prediction of the global CH_4 sources and budget is crucial for policy-making of climate change mitigation (Chang *et al* 2019).

Increasing anthropogenic emissions are responsible for the growing CH_4 levels in the atmosphere (Ghosh *et al* 2015). Among the various human-induced CH_4 sources, livestock production is one of the largest contributors (Reay *et al* 2018), in which emissions from enteric fermentation of ruminants ($CH_{4,ef}$) accounts for approximately 87% of the total livestock emissions (Saunois *et al* 2020). According to the latest Intergovernmental Panel on Climate Change (IPCC) report (IPCC 2022), $CH_{4,ef}$ made up 23% of the more than ten CO_2-equivalent GHG emissions from the agriculture sector per year. Globally, cattle, buffalo, goat and sheep together emit 96% of

$CH_{4,ef}$ (FAO 2006). With the increasing demand for animal products, $CH_{4,ef}$ is growing and this trend is predicted to continue in the future (Dangal *et al* 2017b). Accurate estimation of $CH_{4,ef}$ is of great importance to identify a more realistic definition of the baseline for climate mitigation (Dangal *et al* 2017b), and to better understand the global CH_4 budget (Saunois *et al* 2016).

Our current assessment of CH_4 emissions from livestock relies mainly on the inventory-based models (IvtMs) (Storm *et al* 2012). Using periodically updated emission factors (EFs) and livestock density distributions, the spatio-temporal pattern of livestock CH_4 emissions was predicted globally. Crutzen *et al* (1986) generated one of the first comprehensive assessments of global livestock CH_4 production using regional statistical metrics of associated EFs. This approach was then adopted in the IPCC methodology. With more detailed considerations of livestock physiological conditions and activity scenarios, the IPCC Tier 2 and Tier 3 methods provide more customized estimates following local conditions but requires much more detailed local information (IPCC 2006, IPCC 2019). Various estimations have been made using different data sources. According to the latest assessment, the estimated CH_4 emissions from livestock ranges from 103 to 130 Tg CH_4 yr^{-1} depending on the inventory-based approaches globally (Chang *et al* 2021).

With the recognition of the importance of anthropogenic-related processes in the global carbon budget and carbon-climate feedback, the global vegetation models (GVMs), a typical land component of earth system models (ESMs), are incorporating the land management components. Efforts have been made over the past several decades to introduce the livestock-related processes into GVMs. As summarized by Pongratz *et al* (2018), an increasing number of pasture system models with explicit consideration of livestock processes have been incorporated into GVMs and are supposed to be developed by more model communities in the future. Those models coupled the livestock processes, e.g. direct biomass intake, trampling, and scorching, with vegetation and soil carbon cycling. Examples include the pasture simulation model (PASIM) in ORCHIDEE (Chang *et al* 2013), the defoliate rate model (DRM) in Biome-BGC (Han *et al* 2014), the SAVANNA model (Liedloff *et al* 2001) and the Illius and O'Connor model (IOM) in LPJ-GUESS (Pachzelt *et al* 2015). All these models have already been applied in continental and global land C assessments. Based on this framework, CH_4 emissions were further quantified by converting the biomass or energy intake (Dangal *et al* 2017a). With the increase of model tools, large discrepancies in livestock C uptake predictions (0.1–16.1 gC m^{-2} yr^{-1} over temperate Eurasian Steppe (TES)) were found, possibly leading to divergent predictions of $CH_{4,ef}$ (Chen *et al* 2018). Moreover, such models have rarely been explicitly benchmarked at large scales and therefore, the performances of individual model are still largely unknown.

Despite the different methodologies and protocols being adopted in both IvtMs and process-based models (PcMs), they share a similar target for quantifying and predicting the GHG emissions from the livestock sector. Currently, the two types of approaches have been developed and updated in relatively independent pathways. To date, these approaches and their corresponding outputs have not yet been explicitly compared and analyzed under a unified protocol.

In this study, we presented a comprehensive comparison between the latest IvtMs and PcMs to estimate $CH_{4,ef}$ over the temperate grasslands of Inner Mongolia (IM), a region dominated by typical temperate grasslands that are widely used for animal husbandry. The region was chosen as a suitable testbed for this study due to the plenty background livestock information and dataset, extensive grassland and livestock types, and well validated vegetational model sets. First, various IvtMs were implemented to quantify the regional spatial-explicit $CH_{4,ef}$. Thereafter, the results of different PcMs over the same region were generated using a livestock model comparison platform (Chen *et al* 2018). Finally, the $CH_{4,ef}$ estimates from both groups were explicitly compared and analyzed. Based on the study, we aimed to quantify the differences in modeling $CH_{4,ef}$ from various approaches and sources, and then to identify and understand the sources of model differences.

2. Materials and methods

2.1. Study region

IM is the eastern end of TES. The longitudinal and latitudinal extents are 97°12′–126°04′ E and 37°24′–53°23′ N respectively. The region is dominated by the temperate continental monsoon climate, characterized with short and hot summer, and long and cold winter (Guo *et al* 2021). Grasslands are the dominant vegetation type in IM, which has extensively been used for animal husbandry over hundreds of years (Wang *et al* 2017).

The regional grasslands exhibit a clear decreasing trend of productivity from north-east to south-west, with consecutive changes of grassland types (figure 1). Temperate meadow steppe is mainly distributed in the north-east of IM, with net primary productivity (NPP) generally higher than 220 gC m^{-2}. Temperate typical steppe is the major grassland type in the middle of IM, with NPP generally ranging from 60 gC m^{-2} to 220 gC m^{-2}. Temperate desert steppe is mainly distributed in the south-west of IM, with NPP generally lower than 60 gC m^{-2}.

Various species are extensively held in IM, including ruminants such as cattle, goats, sheep and non-ruminants like horses, donkeys, mules. Sheep,

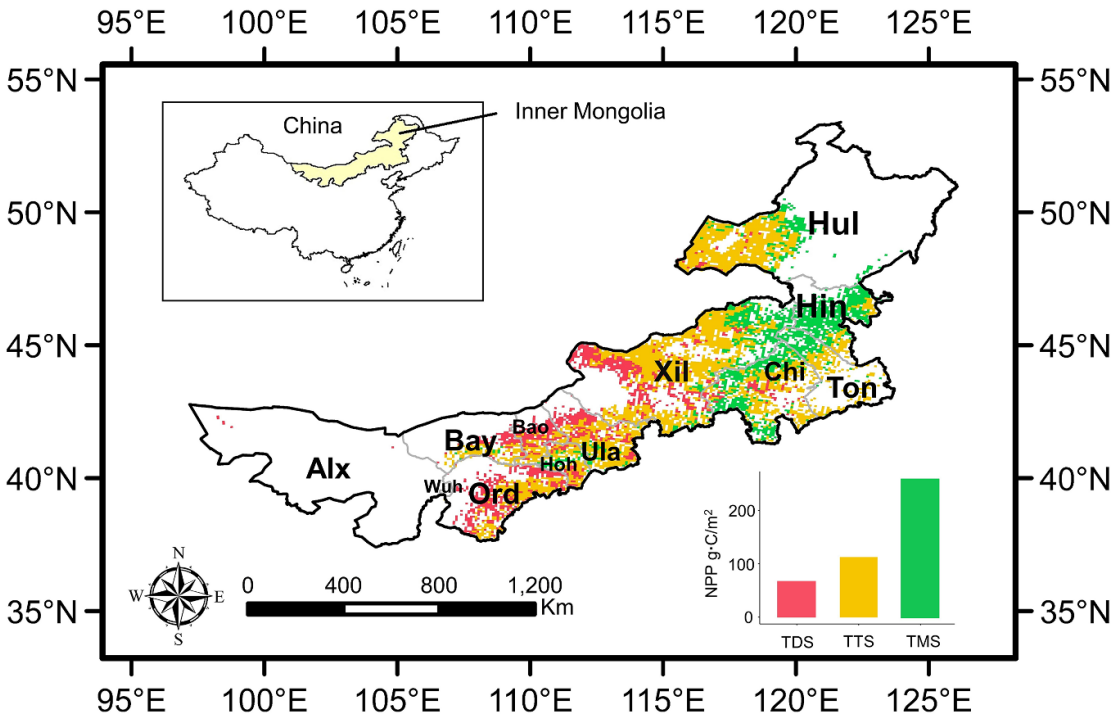

Figure 1. The spatial distribution of grassland types in the study region. TDS: temperate dessert steppe; TTS: temperate typical steppe; TMS: temperate meadow steppe. Hul: Hulunbuir; Hin: Hinggan League; Ton: Tongliao; Chi: Chifeng; Xil: Xilingol League; Ula: Ulanqab; Bao: Baotou; Hoh: Hohhot; Bay: Bayannur; Ord: Ordos; Wuh: Wuhai; Alx: Alxa League.

goats and cattle comprise the major part of livestock in IM, accounting for 60%, 20% and 8% of the total livestock number (in head), respectively (Inner Mongolia Statistical YearBook, 2007).

2.2. Modeling approach and analysis

2.2.1. IvtMs

Five sources of IvtMs, i.e. IPCC default methods Tier 1 and Tier 2 (hereafter T1_06 and T2_06; IPCC 2006), refined IPCC methods (hereafter T1_19 and T2_19; IPCC 2019), mixed IPCC Tier 1 and Tier 2 method (hereafter MT_2019; Chang *et al* 2021), Peng's method (Peng *et al* 2016, Yu *et al* 2018) and the Emissions Database for Global Atmospheric Research (EDGAR) datasets (v2.0, v4.3.2, v5.0 and v6.0, Olivier *et al* 1996, Janssens-Maenhout *et al* 2017, Crippa *et al* 2019), were included in this study. Both methods of Peng and EDGAR follow the IPCC default methods (Peng *et al* 2016, Crippa *et al* 2019) but with customizations. Specifically, Peng's method applied the T2_06 method as the baseline and improved the quantification of EF values with local statistics in China and explicitly considers of the average lifespan of livestock (Peng *et al* 2016, Yu *et al* 2018). The EDGAR versions mainly applied EF values from the IPCC default Tier 1 method and incorporated algorithms from the IPCC default Tier 2 method in recent versions; Crippa *et al* (2019), Oliver *et al* (1996). The livestock distribution map in the EDGAR dataset also changed with corresponding updates from FAO.

Overall, the $CH_{4,ef}$ is calculated using the following equation:

$$CH_{4,ef} = \sum_{i=1}^{N} pop_i \times EF_i \times (ALS_i/12) \quad (1)$$

where pop_i is the population of livestock type i; EF_i is the emission factors of livestock type i (kg CH_4 head^{-1} yr^{-1}); ALS_i is the average lifespan of livestock in a calendar year for livestock type i (month). The ALS factor has not been explicitly considered in any method other than Peng's method, in which ALS for cow, non-dairy cattle and sheep/goat is 12 months, 10 months and 7 months, respectively (Yu *et al* 2018).

For the T1_06 and T1_19 method, the EF_i values from Crutzen *et al* (1986) were adopted for each livestock type. In the T2_06 and T2_19 method, EF_i is calculated as follows:

$$EF_i = \left[\frac{GE_i \times Y_{m,i}\% \times 365}{EC}\right] \quad (2)$$

where GE_i is the gross energy intake of livestock type i per day (MJ head^{-1} d^{-1}) and $Y_{m,i}$% is CH_4 conversion factor of livestock type i, i.e. the percentage of gross intake energy being converted to CH_4. The values were obtained from the IPCC guidelines of 2006 and 2019 (IPCC 2006, IPCC 2019). EC is the energy content of CH_4 and equals 55.65 MJ kg^{-1} of CH_4.

GE_i is calculated as follows:

$$GE_i = \left[\frac{\left(\frac{NE_{m,i}+NE_{a,i}+NE_{l,i}+NE_{work,i}+NE_{p,i}}{REM_i} \right) + \left(\frac{NE_{g,i}+NE_{wool,i}}{REG_i} \right)}{DE_i\%} \right] \quad (3)$$

where $NE_{m,i}$ is the net energy required by the animal for maintenance, MJ d^{-1}; $NE_{a,i}$ is the net energy for activity, MJ d^{-1}; $NE_{l,i}$ is the net energy for lactation, MJ d^{-1}; $NE_{work,i}$ is the net energy for work, MJ d^{-1}; $NE_{p,i}$ is the net energy for pregnancy; $NE_{g,i}$ is the net energy needed for growth, MJ d^{-1}; $NE_{wool,i}$ is the net energy required to produce a year of wool. REM_i is the ratio of net energy available in a diet for maintenance to digestible energy consumed by livestock type i; REG_i is ratio of net energy available for growth in a diet to digestible energy consumed by livestock type i; $DE_i\%$ is the digestible energy expressed as a percentage of gross energy of livestock type i. Both REM_i and REG_i are functions of $DE_i\%$ (table S1). Among the NE terms, $NE_{a,i}$ is a function of the activity coefficient, which varies with the livestock feeding situations (table S2). We adopted the default sets from the IPCC guidelines to the other NE terms for the T2_06 and T2_19 methods.

The MT_2019 method combined the T1_19 and T2_19 methods (IPCC 2019). The EFs of dairy cows, meat and other non-dairy cattle, buffaloes, sheep, and goats were synthesized from the T2_19 method, and EFs of the rest livestock types were from the T1_19 method (Chang *et al* 2021).

In Peng's method, the EF of dairy cattle is based on an exponential relationship with observed milk production (Yu *et al* 2018), instead of a linear relationship used in the T2_06 method. The species-specific ALS factor was explicitly considered to quantify $CH_{4,ef}$, as described above. In addition, the NE terms of sheep and goat were calculated following the T2_06 method but with values of weight and wool production modified based on the local data from the China Agricultural Products Cost-benefit Information Compilation (CAPCIC, Peng_s1) and the Food and Agriculture Organization of the United Nations—China statistical yearbook (FAO-CSY, Peng_s2) (Yu *et al* 2018).

More details of the EF quantification can be found in text S1. All the EFs used in our study were listed in table S3.

For the EDGAR datasets, the livestock distribution map and the method to quantify the EF values are updated with versions. The livestock distribution keeps updating with the outcomes from FAO datasets. Specifically, EDGAR v4.3.2 used livestock distribution from FAO (2014) and EDGAR v5.0 used livestock distribution from FAO (2018). Regarding EF values, EDGAR v2.0 mainly applied a method from IPCC (1997), and the following versions mainly applied the T1_06 method (IPCC, 2006). Further modifications were made to each upcoming version. In the EDGAR v4.3.2, country-specific milk yield and carcass weight were used to quantify the EF values of dairy and non-dairy cattle (Janssens-Maenhout *et al* 2017). In the EDGAR v5.0 and v6.0, the EF values of dairy and non-dairy cattle were further updated following the T2_06 method (Crippa *et al* 2019).

As the PcMs used a unified livestock unit, i.e. sheep unit, to quantify the livestock density distribution in the region (see the corresponding explanation in section 2.2.2), we further calculated the EF values of all IvtMs with sheep unit using the livestock conversion rate provided by FAO (FAO 2006, table S4).

2.2.2. PcMs

Livestock activities are considered as part of the land biogeochemical cycling in the PcMs. They are linked to the vegetational and soil processes through direct biomass intake, excretion, and trampling (Liu *et al* 2015, Vuichard *et al* 2007). To couple with the other land surface processes, such livestock models are generally designed to run at daily or finer temporal resolutions. In this study, the outputs from five PcMs, i.e. the DRM, the IOM, the PASIM, the SAVANNA model and the Shiyomi model (SM), were used.

Livestock activities influence terrestrial C cycling mainly through three processes: direct intake, excretion and trampling (Vuichard *et al* 2007b).

For direct intake, livestock removes biomass from plants and standing litters, causing defoliation and thereafter lower litter input into the soil (Chen *et al* 2018). Three types of algorithms are used in different models. In DRM, the direct intake was considered as a linear relationship between the defoliation rate and the available biomass (No'am *et al* 1992):

$$\frac{dB_{in}}{dt} = pr_{in} \times B_{a,t} \quad (4)$$

where pr_{in} is the potential intake efficiency (m^2 d^{-1} per livestock unit) and $B_{a,t}$ is the available biomass for time t (kg m^{-2}).

SM considers the direct intake through the livestock demand associated with livestock weight (Shiyomi *et al* 2011):

$$\frac{dB_{in}}{dt} = \sum_i W_t \times r_{in,i} \times q_i \quad (5)$$

where W_t is the livestock weight at time t (kg), $r_{in,i}$ is the forage intake rate of composition i (i = live biomass or dead biomass) and q_i is the fraction of composition i. The forage intake is considered as percentage from available biomass once forage availability is limited (table S1).

IOM, PASIM and the SAVANNA model share a similar approach to calculate direct intake:

$$\frac{dB_{in}}{dt} = K_t \times gf \quad (6)$$

where K_t is the intake rate constrained by the forage availability at time t, which is calculated using the Michaelis-Menten (M-M) function:

$$K_t = \frac{I_{max} \times V_t}{(\beta + V_t)} \quad (7)$$

where I_{max} is the intake biomass with maximum consumption ability of livestock (kg d^{-1} per livestock unit). It is a function of livestock mass (A_{HFT}) in IOM but set to constant values in the other two models. V_t is the vegetation abundance at time t (kg m^{-2}). β is the half maximum intake rate (kg m^{-2}).

gf in equation (6) is the other factors regulating the direct intake, such as the age level in IOM and the weight condition in the SAVANNA model.

For livestock excretion, The C return from excretion to soil is represented as a set percentage from livestock intake in SM and DRM. It is calculated as the difference between livestock intake and the sum of other C outputs in PASIM.

The trampling and scorching effect is described as a flux from aboveground C pools to the litter or soil C pools:

$$B_{ts} = n \times p \quad (8)$$

where B_{ts} is the biomass loss from trampling and scorching effect, n is the livestock density (livestock unit m^{-2}) and p is the effect coefficient, equals to 0.008 (kg per livestock unit) (Vuichard *et al* 2007b).

More detailed equations and parameterizations of the PcMs can be found in tables S5 and S6, respectively.

To quantify $CH_{4,ef}$, a conversion rate from the total biomass intake was used. Three from the five models use this method to quantify livestock $CH_{4,ef}$ with a same value of 3% (Minonzio *et al* 1998). In this study, we applied this conversion rate to all the simulations. As some PcMs only provide the sheep-based parameterization, all livestock types were translated into sheep unit based on the conversion rate provided by FAO for the regional study (table S4).

2.3. Data used and processing

The grassland distribution of IM was from the MODIS land cover data set with a grassland classification from National Tibetan Plateau Data Center (Pan *et al* 2021). Livestock distribution was from 'Gridded Livestock of the World' (GLW Ver. 2.0, http://livestock.geo-wiki.org/), which represents the livestock distribution in 2006 (Robinson *et al* 2014). The livestock densities of sheep, goats and cattle were used in this study. The spatial distribution of livestock density was used as the input for both IvtMs and PcMs to quantify total $CH_{4,ef}$ emission from each grassland pixel by multiplying it with $CH_{4,ef}$ of per livestock unit.

The spatial distribution of NPP and aboveground NPP (ANPP) across the study region were obtained from the grassland version of Boreal Ecosystem Productivity Simulator (BEPS), with a spatial resolution of 0.083 33°. The model performance has been extensively validated using *in-situ* observations over the study region and is widely applied in the regional assessments (Chen *et al* 2016, 2017). To run BEPS, leaf area index (LAI), meteorology, CO_2 and soil information are required. LAI was from the GlobalLAI dataset (www.globalmapping.org/globalLAI/). Meteorological data was from Meteorological Forcing Dataset for Land Surface Modeling (http://rda.ucar.edu/datasets/ds314.0/). Atmospheric CO_2 data was from Mauna Loa Observatory, Hawaii (20° N, 156° W) (http://cdiac.esd.ornl.gov/ftp/trends/co2/maunaloa.co2). Soil texture data was from the global soil dataset for use in ESMs (http://globalchange.bnu.edu.cn/research/soilw).

$CH_{4,ef}$ from the EDGAR in 2006 was obtained from the website: https://edgar.jrc.ec.europa.eu. We collected the $CH_{4,ef}$ results from four versions of the EDGAR datasets, i.e. v2.0, v4.3.2, v5.0 and v6.0. The spatial resolution is 0.1° × 0.1° for v4.3.2, v5.0 and v6.0, and 1° × 1° for v2.0.

All spatial-explicit data are for 2006 to match the year of the livestock distribution map. The spatial resolution of the datasets was unified to 0.083 33°.

2.4. Model simulation and comparison

The PcMs were integrated into BEPS. We kept the original parameterizations in each PcM but only made essential modifications to the livestock-type related parameters to sheep unit based values. As the PcMs generally use unified parameterizations for continental or global studies, our analysis in IM can well reflect the model performances at the larger scales.

The age-related factor was considered in IOM, so we undertook four simulations with different age-based parameterizations (i.e. age = 0–1, 1–2, 2–3 and >3). In the SAVANNA model, the initial weight of livestock varied with different management conditions (Christensen *et al* 2003). It was set to three levels (i.e. high initial weight, W_{ini} = 80 kg per sheep unit, medium initial weight, W_{ini} = 60 kg, low initial

weight, W_{ini} = 40 kg) following Chen *et al* (2018). In total, ten simulations were explicitly run for BEPS coupled with the PcMs in this study.

The model was run in a daily step, with a spatial resolution of 0.083 33°. We summarized the accumulated $CH_{4,ef}$ in 2006 from different PcMs to compare with the corresponding outputs from IvtMs.

2.5. Parameter sensitivity analysis

A parameter sensitivity analysis was conducted for the PcMs. All parameters used in each PcMs were tested through the following approach (Williams *et al* 2012):

$$|R| = \frac{\Delta Y}{Y} \times \frac{X}{\Delta X} \quad (9)$$

where $|R|$ is the response coefficient equivalent to relative change in $CH_{4,ef}$ (i.e. $\frac{\Delta Y}{Y}$) caused by the relative change in a parameter (i.e., $\frac{X}{\Delta X}$). In each test, we imposed a 2% increase in the parameter magnitude to calculate the $|R|$ value. A higher value means a higher importance of the parameter to the $CH_{4,ef}$ estimation. Parameters with $|R|$ higher than 0.2 were considered as sensitive.

3. Results

3.1. Spatial distributions of livestock density and ANPP

The spatial distributions of livestock density and grassland productivity were inconsistent across the region. For livestock, the regional mean density of cattle, sheep, and goats were 3.88 head km^{-2}, 55.81 head km^{-2}, and 19.94 head km^{-2}, respectively. The distribution of cattle within the region was more locally concentrated (i.e. >40 head km^{-2}), especially in Hohhot (Hoh), Ulanqab (Ula) and part of Chifeng (Chi) (figure 2(a)), while the distributions of sheep and goats were more dispersed (figures 2(b) and (c)). Sheep were widely distributed over the middle and south-east of IM, with the highest density centers (i.e. >100 head km^{-2}) in the south of Ordos (Ord) and the middle of Ula. Goats were also widespread over the entire region, and at particularly high densities in the middle and east of Ord, the west of Bayannur (Bay), and the north-east of Chi.

Although the total number of sheep and goats each greatly exceeded that of cattle, the spatial distribution of livestock density when converted to sheep unit revealed high density over the south of Ula that more closely resembled the distribution from that of cattle, due to the high conversion rate of cattle (figure 2(d)). Other areas with moderate or high density of sheep unit were over the north-east of Chi and the west of Bay, corresponding to the major centers of sheep and goats distribution.

The regional mean ANPP in 2006 was 58.17 gC m^{-2}, which showed a decreasing spatial trend from the northeast to southwest (figure 2(e)). ANPP was generally higher than 120 gC m^{-2} in temperate meadow grasslands (figure 2(e)), such as the east of Xilingol (Xil), Hulunbuir (Hul), Hinggan (Hin), Tongliao (Ton), and Chifeng (Chi). By contrast, ANPP in barren grasslands, primarily consisting of temperate desert grasslands, was lower than 40 gC m^{-2}, including areas in the west of Bay and Xil and the centers of Ord and Xil.

Latitudinally, productive grasslands were mainly located over high latitude areas with peak ANPP around 45–50° N, while the livestock density gradually decreased from low to high latitude, with the highest distribution in areas with latitude lower than 45° N (figure 2(f)).

3.2. Spatial distribution of predicted $CH_{4,ef}$

For the IvtMs, both the ensemble mean and the individual models of $CH_{4,ef}$ aligned well with the distribution of livestock (figures 3(a) and S1). Moreover, the spatial patterns were very similar between outputs generated using different livestock types and those that used sheep unit (figure 3(b)).

Spatial distribution of the standard deviation (SD) of $CH_{4,ef}$ was generally consistent with that of the mean $CH_{4,ef}$ for the IvtMs (figure 3(d)). In addition, inter-model differences were greater over areas with high sheep density than those with high cattle density, e.g. grasslands over the south of Ula and Hoh, indicating greater differences in the quantification of $CH_{4,ef}$ from sheep than that of cattle. This conclusion was supported by the SD distribution of sheep unit, in which all areas with high livestock density showed large discrepancies between models (figure 3(e)).

The coefficient of variation (CV) values of the IvtMs were generally lower than 0.5 (figure 3(g)), Only scattered areas in Hul presented CV values higher than 1.0. Since a unified livestock index was used for these analyses, the SD map of $CH_{4,ef}$ obtained using sheep unit was generally similar to the map of mean CV, with small, local variations (figure 3(h)).

We then examined the spatial distribution of mean $CH_{4,ef}$ from PcMs. The results showed that, geographically, mean $CH_{4,ef}$ more closely resembled ANPP distribution than the livestock density distribution (figures 2(e) and 3(c)). Similar to ANPP, the average $CH_{4,ef}$ in PcMs exhibited a decreasing tendency from north-east to south-west, with high $CH_{4,ef}$ (>0.6 g CH_4/m^2 yr) areas located over productive grasslands. The SD distribution of $CH_{4,ef}$ aligned well with maps of mean value, which reflected a close positive relationship between the absolute difference among individual PcM and absolute predicted $CH_{4,ef}$ levels (figure 3(f)).

The CV values from PcMs were generally higher than 0.9, with high CV values (> 1.6) areas largely in productive areas (figure 3(i)). In particular, individual models with low $CH_{4,ef}$ predictions more closely followed patterns of livestock distribution, whereas models with high $CH_{4,ef}$ predictions

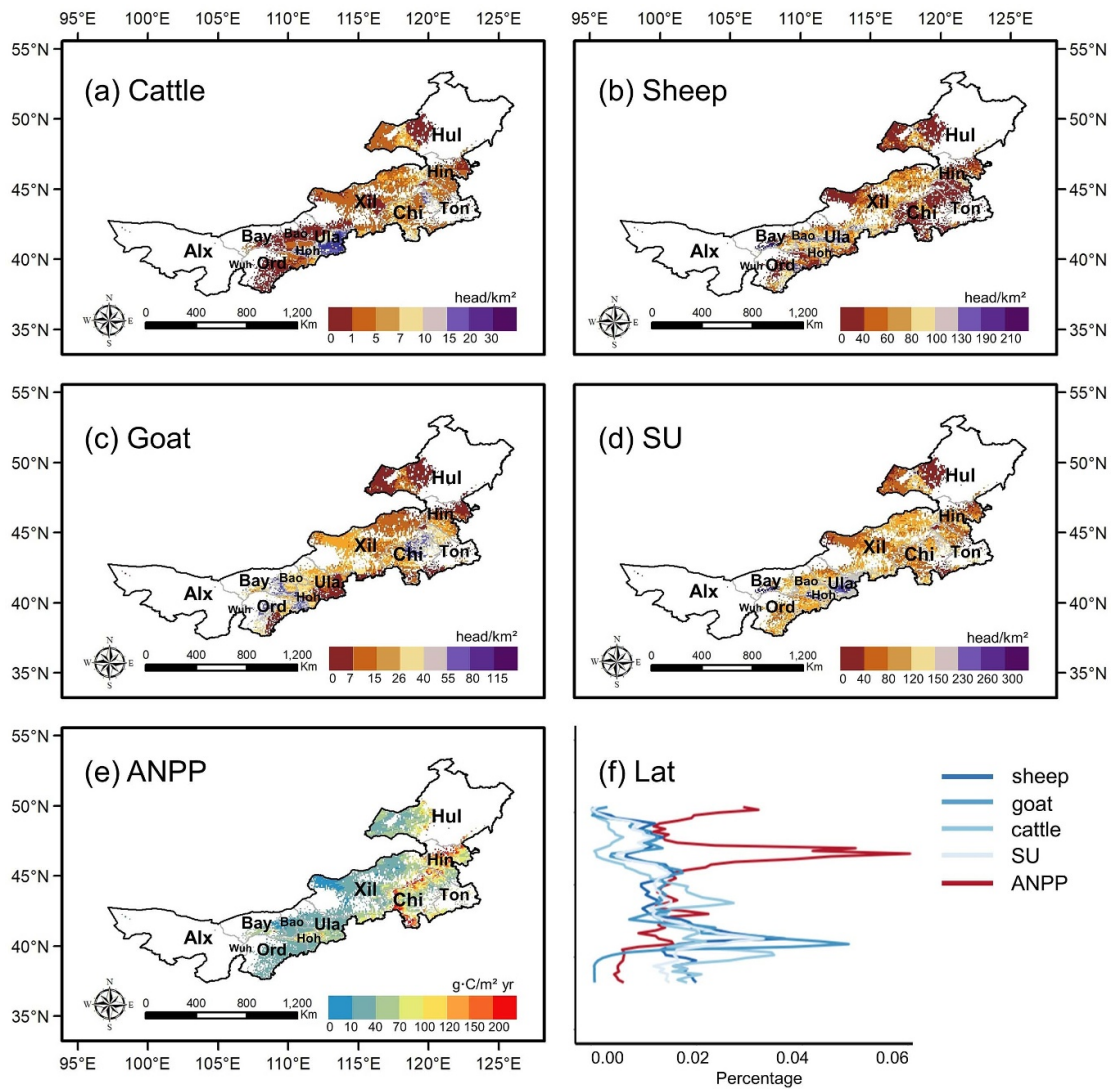

Figure 2. The spatial distributions of livestock (a) cattle, (b) sheep, (c) goat, (d) livestock density using sheep unit (SU); and (e) aboveground net primary productivity (ANPP) over the study region; (f) latitude distribution of ANPP, sheep, goats, cattle and SU, with a bin of 1°. Hul: Hulunbuir; Hin: Hinggan League; Ton: Tongliao; Chi: Chifeng; Xil: Xilingol League; Ula: Ulanqab; Bao: Baotou; Hoh: Hohhot; Bay: Bayannur; Ord: Ordos; Wuh: Wuhai; Alx: Alxa League.

appeared to reflect constraints introduced by differences in resource availability (figure 3).

The PcMs prediction of seasonal variations in $CH_{4,ef}$ further showed a transition from patterns determined by demand in growing seasons to patterns determined by resource limitations in non-growing seasons (figure 4). At the beginning of the year, $CH_{4,ef}$ from all models were highly constrained by forage availability, generating similar low $CH_{4,ef}$ for different models from January to April. The resource limitation was gradually alleviated after April, with increasing grassland productivity. During the growing season, $CH_{4,ef}$ predictions presented a high divergence between models, with different estimations of forage demand. Finally, increases of $CH_{4,ef}$ slowed down after September due to the decrease of available resources. Such a seasonal pattern of $CH_{4,ef}$ is particularly clear for models with high estimations. For example, $CH_{4,ef}$ from DRM followed a seasonal trend that corresponded to the high similarity in spatial distribution between ANPP and $CH_{4,ef}$ (figure S3(h)).

3.3. Parameter sensitivity of the PcMs

Parameter sensitivity analysis indicated that $CH_{4,ef}$ estimations from the PcMs is mainly controlled by the direct intake process (table 1). In all models, the parameters defining the potential or actual intake rates exhibit very close relationships with the $CH_{4,ef}$ outputs from the corresponding models. For the models using the M-M function to quantify livestock direct intake, the half maximum intake rate (β in IOM and the SAVANNA model and equivalent to K^q in PASIM) is another common sensitive parameter. The $|R|$ values for β are similar in IOM (0.40) and the SAVANNA model (0.51), while the related parameters to calculate β is much higher for PASIM as an exponential function is used. In addition, the $CH_{4,ef}$

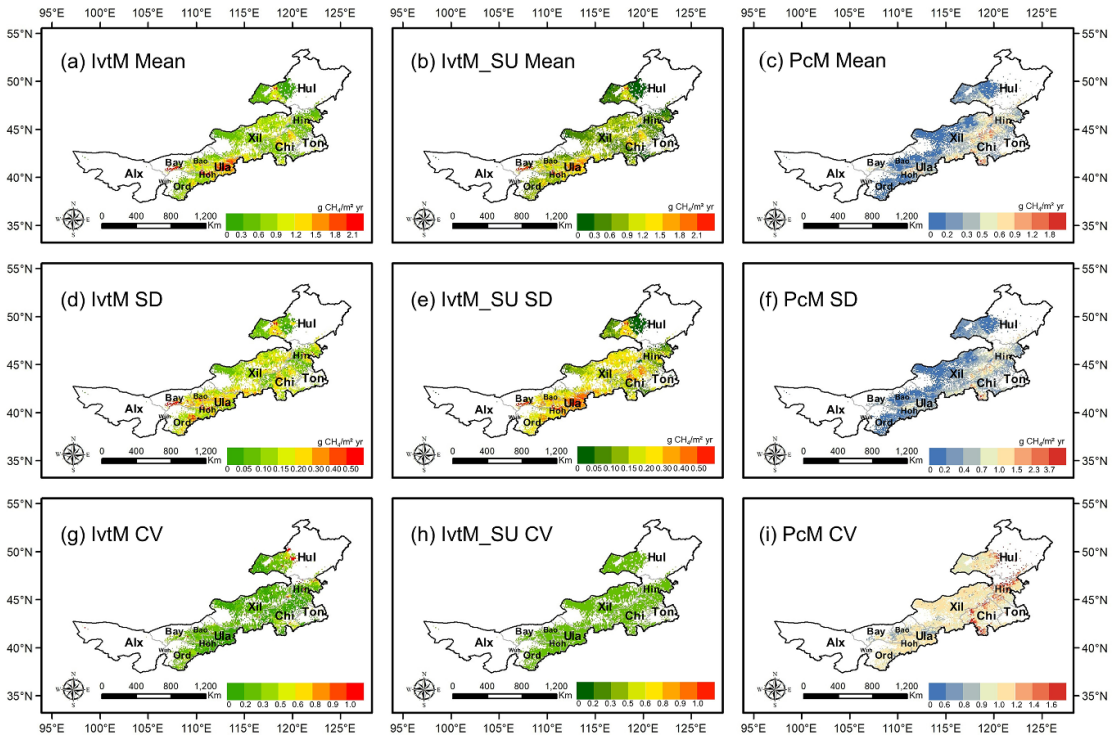

Figure 3. The spatial distributions of (a) ensemble mean $CH_{4,ef}$ of inventory-based models (IvtM Mean); (b) ensemble mean $CH_{4,ef}$ of inventory-based models using sheep unit (IvtM_SU Mean); (c) mean $CH_{4,ef}$ of Process-based models (PcM Mean); (d) standard deviation (SD) of $CH_{4,ef}$ of IvtMs (IvtM SD); (e) SD of of $CH_{4,ef}$ InvMs (IvtM_SU SD); (f) SD of $CH_{4,ef}$ of PcMs (PcM SD); (g) CV of $CH_{4,ef}$ of IvtMs (IvtM CV); (h) CV of $CH_{4,ef}$ of IvtM SU (IvtM_SU CV); (i) CV of $CH_{4,ef}$ of PcMs (PcM CV). Hul: Hulunbuir; Hin: Hinggan League; Ton: Tongliao; Chi: Chifeng; Xil: Xilingol League; Ula: Ulanqab; Bao: Baotou; Hoh: Hohhot; Bay: Bayannur; Ord: Ordos; Wuh: Wuhai; Alx: Alxa League.

output of the SAVANNA model is also highly sensitive to the weight-related parameters.

3.4. IvtMs vs PcMs

Finally, we compared the predicted $CH_{4,ef}$ between IvtMs and PcMs. For most areas, mean $CH_{4,ef}$ from the IvtMs was higher than those from the PcMs (figure 5). Areas with the most distinguishing differences (<-1.2 g CH_4/m^2 yr) were mainly in the southwest of IM (figure 5(a)). CV of $CH_{4,ef}$ from the IvtMs was generally lower than that from the PcMs (figure 5(b)). Moreover, the ratio of mean $CH_{4,ef}$ of PcMs to IvtMs ($R_{PcMs/IvtMs}$) was lower than 0.6 for most areas, and only over the most productive, $R_{PcMs/IvtMs}$ can be higher than 1.0 (figure 5(c)).

Regionally, the ensembled mean $CH_{4,ef}$ from IvtMs was approximately twice larger than that from PcMs and with a much less inter-model difference (0.78 ± 0.14 g CH_4/m^2 yr for IvtMs and 0.34 ± 0.36 g CH_4/m^2 yr for PcMs). Among the IvtMs predictions, outputs from models using sheep unit showed slightly higher mean $CH_{4,ef}$ and larger SD (0.79 ± 0.23 g CH_4/m^2 yr) than the ones using varied livestock types (figure 6(a)).

Within the IvtMs, minor $CH_{4,ef}$ difference was found between the outputs from the IPCC methods of 2006 and the updated ones of 2019 in the study region (figure 6(b)). Generally, outputs with IPCC Tier 2 method predicted higher $CH_{4,ef}$ than the ones using the Tier 1 method. The T2_2019 method predicted the highest $CH_{4,ef}$ among the IvtMs using varied livestock types, with a value of 0.90 ± 0.08 g CH_4/m^2 yr. While the lowest prediction was from the Peng_s2 method, with a value of 0.56 g CH_4/m^2 yr. The sheep unit based outputs for the IPCC Tier 1 and Tier 2 methods showed lower and higher $CH_{4,ef}$ comparing to the outputs from models that used varied livestock types, respectively. Predicted $CH_{4,ef}$ from EDGAR versions ranged from 0.58 to 0.73 g CH_4/m^2 yr, which was slightly higher than the IPCCT1_2006 outputs but lower than the outputs from the IPCC Tier 2 method.

In contrast, outputs of PcMs showed much larger discrepancies among each other. Results from the SAVANNA, SM and PASIM simulations were much lower than the inventory-based outputs, suggesting that those models potentially under-estimated $CH_{4,ef}$. Outputs from the IOM simulations were closer to the average level of the inventory-based outputs. Specifically, the IOM_0_1 and IOM_1_2 simulations predicted slightly lower $CH_{4,ef}$ than the lowest result from IvtMs, i.e. 0.47 g·CH_4/m^2 yr, while the IOM_2_3 and IOM_3more predicted slightly higher $CH_{4,ef}$. The DRM simulation predicted a higher value, i.e. 1.19 g CH_4/m^2 yr, than all the inventory-based predictions.

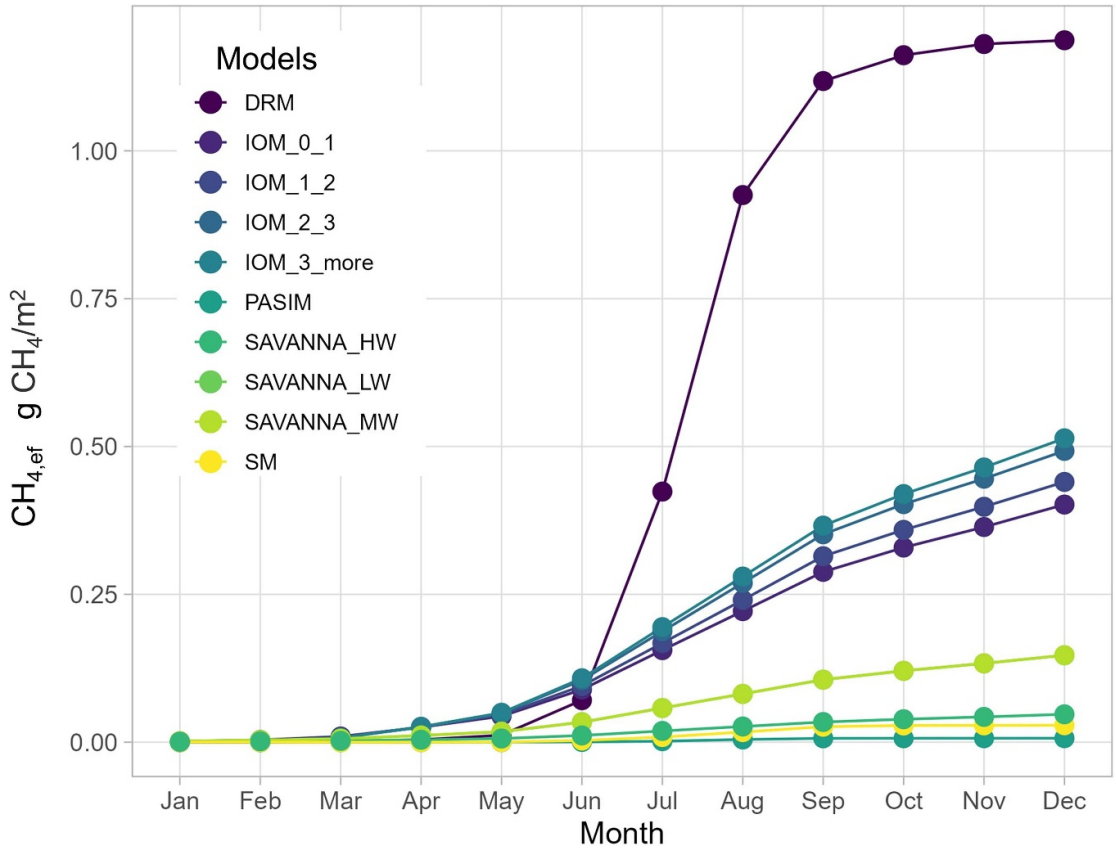

Figure 4. The seasonal pattern of CH_4 emissions from livestock enteric fermentation ($CH_{4,ef}$) predicted from the process-based models (PcMs).

Table 1. The sensitive parameters in different process-based models to estimate $CH_{4,ef}$.

DRM[a]		PASIM[b]		SM[c]		IOM[d]		The SAVANNA model[e]	
Name	$\|R\|$	Name	$\|R\|$	Name	$\|R\|$	Name	$\|R\|$	Name	$\|R\|$
pr_{in}	0.85	q	2.65	r_{in}	0.73	A_{HFT}	0.83	I_{max}	0.91
V_r	0.73	K	1.38	W_{max}	0.24	m	0.51	W_{ini}	0.81
		I_{max}	0.63	W_{ini}	0.21	β	0.40	W_{max}	0.77
						M_j	0.23	β	0.51
								W_{min}	0.34

[a] DRM, pr_{in}: potential intake efficiency, Vr: residual aboveground biomass.

[b] PASIM, q: intake parameter, K: leaf area index related intake parameter, I_{max}: maximum livestock intake rate.

[c] SM, r_{in}: actual intake rate as a fraction of animal weight, W_{max}: maximum weight over a year, W_{ini}: initial weight at the beginning of the year.

[d] IOM, A_{HFT}: mature mass per livestock unit, m: metabolic coefficient, β: half maximum intake rate, M_j: ratio of body mass in an age class from mature mass.

[e] The SAVANNA model: I_{max}: same as the one from PASIM, W_{ini}: same as the one from SM, W_{max}: same as the one from SM, β: same as the one from IOM, W_{min}: minimum weight over a year.

4. Discussion

As the most important anthropogenic CH_4 source, livestock CH_4 emissions have been widely investigated and studied. However, to our knowledge, the two major model approaches, the IvtMs and PcMs, have not been explicitly compared and evaluated. Thus, our study provides the first quantitative results to illustrate the model differences within and between approaches over the typical temperate grasslands and explain the source of these differences.

All the IvtMs used in our study follow a unified schematic framework based on the IPCC default method (IPCC 2006, 2019). Different predictions of $CH_{4,ef}$ between IvtMs could be attributed to two sources: the EF per livestock unit and the livestock density. Because unified livestock population distribution data were used in this study (except the EDGAR dataset), the $CH_{4,ef}$ difference between the IvtMs was mostly from the EF values.

We found higher predicted $CH_{4,ef}$ from the models based on IPCC Tier 2 method than those from

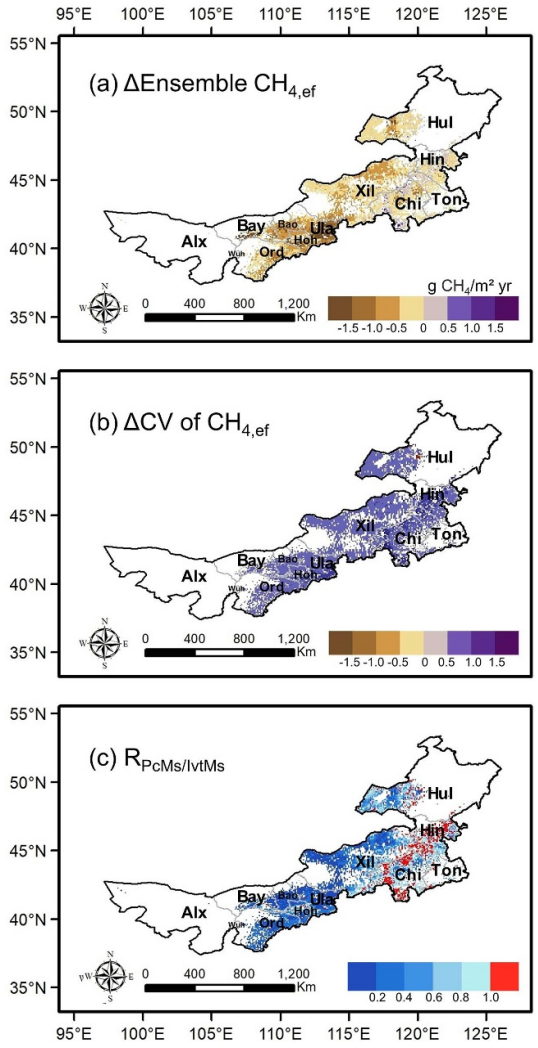

Figure 5. The spatial distributions of (a) difference of mean $CH_{4,ef}$ between process-based models (PcMs) and inventory-based models (IvtMs); (b) difference of coefficient of variance (CV) between PcMs and IvtMs. Positive values indicate that the ensembled mean CV values of PcMs is higher than those for IvtMs and negative values indicate that the ensembled mean or CV values of PcMs are lower than IvtMs; (c) the ratio of mean $CH_{4,ef}$ of PcMs to IvtMs ($R_{PcMs/IvtMs}$). Hul: Hulunbuir; Hin: Hinggan League; Ton: Tongliao; Chi: Chifeng; Xil: Xilingol League; Ula: Ulanqab; Bao: Baotou; Hoh: Hohhot; Bay: Bayannur; Ord: Ordos; Wuh: Wuhai; Alx: Alxa League.

IPCC Tier 1 method over the region. This is mainly due to the higher EF values of sheep and goats than cattle in the IPCC Tier 2 method (table S3). Mainly due to an extra consideration of ALS of different livestock types, Peng's method produced lower $CH_{4,ef}$ than the other IPCC Tier 2 based methods in the study region. The EDGAR datasets predicted medium $CH_{4,ef}$ among the IvtMs, which lies between the values from IPCC Tier 1 and Tier 2 methods. This result is reasonable because the EDGAR versions updated EF values and livestock distribution maps using the IPCC default methods and GLW data series respectively; Crippa *et al* (2019), Olivier *et al* (1996), which lead to different combination of EF and livestock distribution compared to the other models used in our study.

To capture the seasonal variations of livestock-related C budget linked to its environment, PcMs generally characterized livestock activities from forage intake and digestion to excretion with finer temporal resolutions than IvtMs. Once incorporated into terrestrial biogeochemical models, the dynamics of livestock, vegetation and soil are coupled. However, owing to the different details of characterizing the processes and parameterization, PcMs deliver diverse results. In general, the forage intake in PcMs is a function that considers the potential livestock intake, i.e. the forage demand, and the biomass abundance, i.e. the resource availability (Fryxell 1991). At the demand end, the optimal intake rate or efficiency is the parameter that generally determines the up limit of livestock forage need and therefore is closely related to the $CH_{4,ef}$ prediction in each PcM (table 1). A relatively high grazing efficiency (pr_{in}) set in DRM probably led to its greatest $CH_{4,ef}$ prediction within the PcMs (Chen *et al* 2018). Among the models using the M-M function, IOM simulations with higher values of maximum intake rate (I_{max}) predicted greater $CH_{4,ef}$ than PASIM and the SAVANNA model. In addition, the physiological condition of livestock is another cause of the divergent predictions. The range of $CH_{4,ef}$ can be more than 0.1 g $CH_{4,ef}$ /m^2 yr under different livestock age or weight levels (table S7). At the resource end, the current PcMs mainly consider the quantity of above-ground vegetational biomass as a scalar of forage availability. Once the livestock demand exceeds the local biomass abundance, the instantaneous forage intake by livestock can be constrained. Spatially, high dependence between the resource availability and $CH_{4,ef}$ was found for models with high forage demand, e.g. DRM (figure S3). While models with low forage demand such as the SM and the SAVANNA model showed a similar spatial pattern to livestock density. For the IOM with different sets of age levels, the spatial distributions of $CH_{4,ef}$ were more livestock density dependent and were also limited by resource availability (figure S3).

Different model strategies for quantifying $CH_{4,ef}$ contribute to the differences of both the regional mean and spatial pattern between the two model groups. The prediction of the IvtMs is mainly from the perspective of livestock demand, with a comprehensive representation of energy costs from various activities and scenarios. While many variables and the corresponding parameterization are given as constants and therefore can hardly capture the potential inter-annual or seasonal variabilities of those factors (Dangal *et al* 2017a). In other words, the IvtMs estimate the expected $CH_{4,ef}$ with forage demand satisfied under certain conditions at a yearly step. For the PcMs, the predicted $CH_{4,ef}$ is a result of both livestock demand and local resource availability and the dynamics of $CH_{4,ef}$ can be explicitly considered and

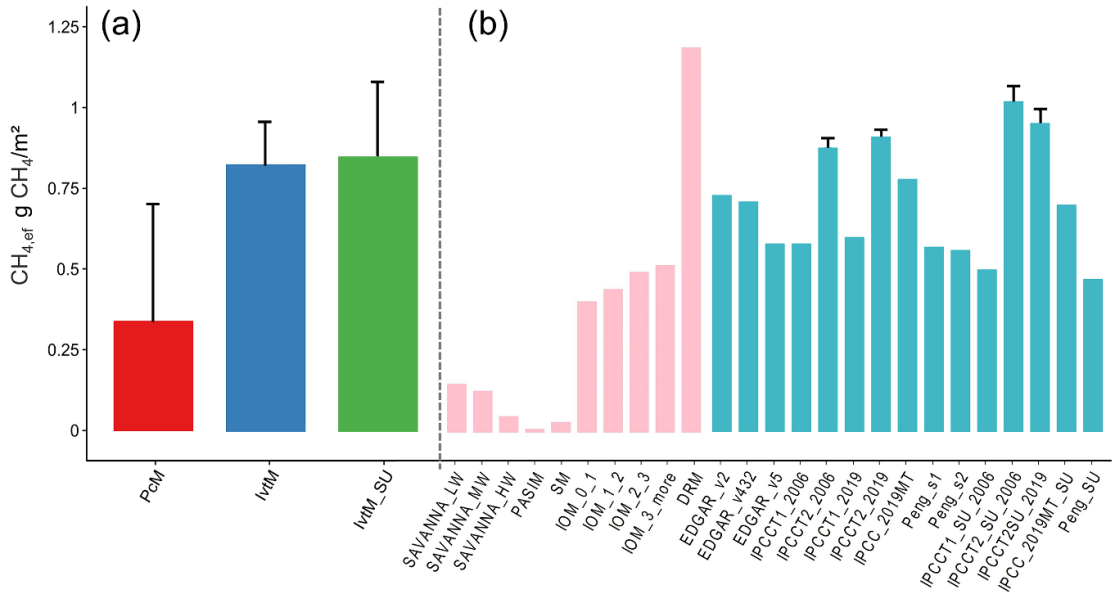

Figure 6. Regional $CH_{4,ef}$ of different models: (a) a comparison of the ensembled $CH_{4,ef}$ between process-based models (PcM), inventory-based models (IvtM) and inventory-based models using sheep unit (IvtM_SU); (b) a comparison of individual models. SAVANNA_LW: SAVANNA model with the low initial weight; SAVANNA_MW: SAVANNA model with the medium initial weight; SAVANNA_HW: SAVANNA model with the high initial weight; IOM_0_1: IOM with a parameterization of livestock age 0–1, IOM_1_2: IOM with a parameterization of livestock age 1–2; IOM_2_3: IOM with a parameterization of livestock age 2–3; IPCCT1_2006: IPCC Tier 1 method based on IPCC (2006); IPCCT2_2006: mean values of IPCC Tier 2 methods based on IPCC (2006); IPCCT1_2019: IPCC Tier 1 method based on IPCC (2019); IPCCT2_2019: mean values of IPCC Tier 2 methods based on IPCC (2019); IPCC_2019MT: the mixed tier approach from Chang; Peng_s1: Peng's method scenario 1; Peng_s2: Peng's method scenario 2; IPCCT1_SU_2006: IPCC Tier 1 based on IPCC 2006 using sheep unit; IPCCT2_SU_2006: the mean value of IPCC Tier 2 method based on IPCC 2006 with using sheep unit; IPCCT2SU_2019: the mean value of IPCC Tier 2 method based on IPCC 2019 using sheep units; IPCC_2019MT_SU: the mixed tier approach from Chang using sheep unit; Peng_SU: Peng's method using sheep unit. The error bars represent 1 SD.

updated by simulating the energy balance between input and output. The description for different sources and costs of energy was less detailed than for the IvtMs, potentially due to a lack of usable data source with compatible spatio-temporal resolution to the GVMs. Due to the constraint from the local resource, we observed a clear seasonality of $CH_{4,ef}$ from the PcMs or areas with high predictions of $CH_{4,ef}$, corresponding to the seasonality of grassland productivity (figure 4). Such a pattern reflects the situation of traditional nomadic-based animal husbandry, in which forage demand could hardly be satisfied during the non-growing seasons, and probably induce corresponding variability on livestock population caused by high mortality rate over winters (Otani *et al* 2016). However, under modern management, the forage sources are not only dependent on local forage availability in grasslands. The development of forage commerce and the wide utilization of forage bars can secure the forage source over non-growing seasons (Wang *et al* 2017). For example, the cultivation area of greenfolder was 634 000 hectares in 2006 and the area of planted grasslands was 1475 300 hectares in IM, which produced 11 995 400 tons of harvested grass (IM Yearbook 2007). Building such infrastructure systems substantially mitigate forage deficits during non-growing seasons or periods with low production during the growing seasons (Wang *et al* 2017). Thus, predictions from both IvtMs and PcMs provide useful scalars to quantify $CH_{4,ef}$ under different management scenarios. $CH_{4,ef}$ should be closer to the estimations from IvtMs over areas under a modern strategy of animal husbandry, whereas it should be closer to the estimations from PcMs over areas under a more traditional strategy. Therefore, we argue that knowing the local management level and strategy is important to accurately predict the spatial distribution and potentially the long-term trend of livestock CH_4 emissions.

Despite the strategy-dependent discrepancy, the $CH_{4,ef}$ predictions from IvtMs and PcMs should be of a similar order of magnitude. Using outputs from IvtMs as the baseline datasets, we suggest that the DRM probably over-estimated the regional $CH_{4,ef}$ with a value even higher than all the IvtMs. Models such as the PASIM and the SM should under-estimate $CH_{4,ef}$ (figure 6). Based on our regional comparison, outputs from the IOM seem more reasonable than those from the other PcMs. Meanwhile, it is noteworthy that all the PcMs used default parameterization based on the model sources, in which the models were evaluated over different sites and regions. Therefore, accurate evaluation of the spatio-temporal patterns of $CH_{4,ef}$ would require more *in situ* observations to be available. Recent development and setup of observations from

non-invasive measurements (Negussie *et al* 2017, Flesch *et al* 2018, Rey *et al* 2019), eddy covariance (Tallec *et al* 2012, Prajapati and Santos 2018) and isotope signature (Klevenhusen *et al* 2010, Chang *et al* 2019) will provide opportunities to better evaluate and benchmark PcMs at large scales. The output will facilitate the enhancement of our ability to predict future $CH_{4,ef}$ and its impact on the C-climate feedbacks.

Finally, both IvtMs and PcMs adopted constant $CH_{4,ef}$ conversion ratio. However, the conversion rate in reality is highly dependent on forage digestibility, which is co-determined by the livestock species, forage composition and quality, growing period of forage and so on (Bruinenberg *et al* 2002, IPCC 2006). Empirically, the forage digestibility ranges from 55% to 65% for good pastures, well preserved approaches and grain supplemented forage-based diets but can be much lower with poor quality forages (IPCC 2006). Thus, an explicit consideration of the variations in digestibility will enhance model performance.

Although contrasting methodologies are implemented by the two model groups, both outputs are informative to the agricultural management and mitigation policy making. With a detailed description of livestock demand, the IvtMs provide straightforward and reliable baseline statistics of $CH_{4,ef}$ for both scientists and decision-makers. Meanwhile, results from the PcMs provide additional insights into the trade-off between local livestock demand and resource availability. The comparison of the spatio-temporal patterns from the two model groups can assist the identifications of local resource deficiency and commercial forage supply requirements. The combined information thus benefits a proper decision making with a comprehensive consideration of food security, ecosystem sustainability and mitigation needs (Smith *et al* 2013). Nevertheless, our results stressed that essential model calibrations and validations are highly needed, especially for those critical processes and the affiliated parameterizations in the PcMs. This study can improve the understanding of both types of models, which will facilitate a more accurate assessment of CH_4 emission from pasture ecosystems and better representation of CH_4 emission in ESMs in the future.

Data availability statement

The data that support the findings of this study are available upon reasonable request from the authors.

Acknowledgments

This study is supported by the National Key Research and Development Program of China (2021YFD02200403), the National Science Foundation of China (32071594, 41701227) and the Priority Academic Program Development of Jiangsu Higher Education Institutions (PAPD). The work of Pavel Groisman is partially supported by the NSF Grant #2020404 'Belmont Forum Collaborative Research: Coastal OceAn SusTainability in Changing Climate' and by NOAA through the Cooperative Institute for Satellite Earth System Studies under Cooperative Agreement NA19NES4320002.

We acknowledge Jinfeng Chang from Zhejiang University, and Shushi Peng from Peking University, for providing their datasets and constructive suggestions for this study. We acknowledge all the other producers and providers of datasets we used in this study.

ORCID iDs

Yizhao Chen https://orcid.org/0000-0002-9218-6679
Pavel Groisman https://orcid.org/0000-0001-6255-324X

References

Bruinenberg M H, Valk H, Korevaar H and Struik P C 2002 Factors affecting digestibility of temperate forages from seminatural grasslands: a review: digestibility of temperate forages from seminatural grasslands *Grass Forage Sci.* **57** 292–301

Chang J F *et al* 2013 Incorporating grassland management in ORCHIDEE: model description and evaluation at 11 eddy-covariance sites in Europe *Geosci. Model Dev.* **6** 2165–81

Chang J, Peng S, Ciais P, Saunois M, Dangal S R S, Herrero M, Havlík P, Tian H and Bousquet P 2019 Revisiting enteric methane emissions from domestic ruminants and their $\delta^{13}C_{CH4}$ source signature *Nat. Commun.* **10** 3420

Change I P O 2006 *IPCC guidelines for national greenhouse gas inventories* 1535 (IPCC)

Change–IPCC Intergovernmental Panel On Climate 2019 *Refinement to the 2006 IPCC Guidelines for National Greenhouse Gas Inventories* (Switzerland: IPCC)

Chen Y, Ju W, Groisman P, Li J, Propastin P, Xu X, Zhou W and Ruan H 2017 Quantitative assessment of carbon sequestration reduction induced by disturbances in temperate Eurasian steppe *Environ. Res. Lett.* **12** 115005

Chen Y, Mu S, Sun Z, Gang C, Li J, Padarian J, Groisman P, Chen J and Li S 2016 Grassland carbon sequestration ability in China: a new perspective from terrestrial aridity zones *Rangel. Ecol. Manage.* **69** 84–94

Chen Y, Tao Y, Cheng Y, Ju W, Ye J, Hickler T, Liao C, Feng L and Ruan H 2018 Great uncertainties in modeling grazing impact on carbon sequestration: a multi-model inter-comparison in temperate Eurasian Steppe *Environ. Res. Lett.* **13** 075005

Christensen L, Coughenour M B, Ellis J E and Chen Z 2003 Sustainability of Inner Mongolian grasslands: application of the Savanna model *Rangel. Ecol. Manage. J. Range Manage. Arch.* **56** 319

Crippa M, Oreggioni G, Guizzardi D, Muntean M, Schaaf E, Lo Vullo E, Solazzo E, Monforti-Ferrario F, Olivier J G J and Vignati E 2019 European Commission, Joint Research Centre) Fossil CO_2 and GHG emissions of all world countries: 2019 report

Crutzen P J, Aselmann I and Seiler W 1986 Methane production by domestic animals, wild ruminants, other herbivorous fauna, and humans *Tellus* B **38B** 271–84

Dangal S R S, Tian H, Lu C, Ren W, Pan S, Yang J, Di Cosmo N and Hessl A 2017a Integrating herbivore population dynamics into a global land biosphere model: plugging

animals into the earth system: plugging animals into the earth system *J. Adv. Model. Earth Syst.* **9** 2920–45
Dangal S R S, Tian H, Zhang B, Pan S, Lu C and Yang J 2017b Methane emission from global livestock sector during 1890–2014: magnitude, trends and spatiotemporal patterns *Glob. Change Biol.* **23** 4147–61
Flesch T K, Basarab J A, Baron V S, Wilson J D, Hu N, Tomkins N W and Ohama A J 2018 Methane emissions from cattle grazing under diverse conditions: an examination of field configurations appropriate for line-averaging sensors *Agric. For. Meteorol.* **258** 8–17
Fryxell J M 1991 Forage quality and aggregation by large herbivores *Am. Nat.* **138** 478–98
Ghosh A *et al* 2015 Variations in global methane sources and sinks during 1910–2010 *Atmos. Chem. Phys.* **15** 2595–612
Guo D, Song X, Hu R, Cai S, Zhu X and Hao Y 2021 Grassland type-dependent spatiotemporal characteristics of productivity in Inner Mongolia and its response to climate factors *Sci. Total Environ.* **775** 145644
Han Q, Luo G, Li C and Xu W 2014 Modeling the grazing effect on dry grassland carbon cycling with Biome-BGC model *Ecol. Complex* **17** 149–57
Janssens-Maenhout G 2017 EDGAR v4.3.2 Global Atlas of the three major greenhouse gas emissions for the period 1970–2012. Data, algorithms, and models Earth Syst. Sci. Data **11** 959–1002
Klevenhusen F, Bernasconi S M, Kreuzer M and Soliva C R 2010 Experimental validation of the Intergovernmental Panel on Climate Change default values for ruminant-derived methane and its carbon-isotope signature *Anim. Prod. Sci.* **50** 159
Liedloff A C, Coughenour M B, Ludwig J A and Dyer R 2001 Modelling the trade-off between fire and grazing in a tropical savanna landscape, northern Australia *Environ. Int.* **27** 173–80
Minonzio G, Grub A and Fuhrer J 1998 *Methan-Emissionen der schweizerischen Landwirtschaft: Quellen und Senken im ländlichen Raum* (Switzerland: Bundesamt für Umwelt, Wald und Landschaft (BUWAL))
Montzka S A, Dlugokencky E J and Butler J H 2011 Non-CO_2 greenhouse gases and climate change *Nature* **476** 43–50
Negussie E, Lehtinen J, Mäntysaari P, Bayat A R, Liinamo A-E, Mäntysaari E A and Lidauer M H 2017 Non-invasive individual methane measurement in dairy cows *Animal* **11** 890–9
Otani S, Onishi K, Kurozawa Y, Kurosaki Y, Bat-Oyun T, Shinoda M and Mu H 2016 Assessment of the effects of severe winter disasters (*Dzud*) on public health in Mongolia on the basis of loss of livestock *Disaster Med. Public Health Prep.* **10** 549–52
Pachzelt A, Forrest M, Rammig A, Higgins S I and Hickler T 2015 Potential impact of large ungulate grazers on African vegetation, carbon storage and fire regimes: grazer impacts on African savannas *Glob. Ecol. Biogeogr.* **24** 991–1002
Peng S *et al* 2016 Inventory of anthropogenic methane emissions in mainland China from 1980 to 2010 *Atmos. Chem. Phys.* **16** 14545–62
Peng S, Piao S, Bousquet P, *et al.* Inventory of anthropogenic methane emissions in mainland China from 1980 to 2010[J]. *Atmospheric Chemistry and Physics*, 2016, **16**(22): 14545-14562.
Pongratz J *et al* 2018 Models meet data: challenges and opportunities in implementing land management in Earth system models *Glob. Change Biol.* **24** 1470–87
Pörtner H O *et al* 2022 *Climate Change 2022: Impacts, Adaptation and Vulnerability* (Switzerland: IPCC)
Prajapati P and Santos E A 2018 Estimating methane emissions from beef cattle in a feedlot using the eddy covariance technique and footprint analysis *Agric. For. Meteorol.* **258** 18–28
Reay D S, Smith P, Christensen T R, James R H and Clark H 2018 Methane and global environmental change *Annu. Rev. Environ. Resour.* **43** 165–92
Rey R, Atxaerandio A, Ruiz R, Ugarte U, González-Recio G-R, Garcia-Rodriguez G-R and Goiri G 2019 Comparison between non-invasive methane measurement techniques in cattle *Animals* **9** 563
Robinson T P *et al* 2014 Mapping the global distribution of livestock *PLoS One* **9** e96084
Saunois M *et al* 2016 The global methane budget 2000–2012 *Earth Syst. Sci. Data* **8** 697–751
Saunois M *et al* 2020 The global methane budget 2000–2017 *Earth Syst. Sci. Data* **12** 1561–623
Smith P, Haberl H, Popp A, Erb K, Lauk C, Harper R, Tubiello F N, de Siqueira Pinto A, Jafari M and Sohi S 2013 How much land-based greenhouse gas mitigation can be achieved without compromising food security and environmental goals? *Glob. Change Biol.* **19** 2285–302
Steinfeld H, Gerber P and Wassenaar T D 2006 *Livestock's Long Shadow: Environmental Issues and Options* (Food and Agriculture Organization)
Storm I M L D, Hellwing A L F, Nielsen N I and Madsen J 2012 Methods for measuring and estimating methane emission from ruminants *Animals* **2** 160–83
Tallec T, Klumpp K, Hensen A, Rochette Y and Soussana J-F 2012 Methane emission measurements in a cattle grazed pasture: a comparison of four methods *Biogeosci. Discuss.* **9** 14407–36
Wang Z, Deng X, Song W, Li Z and Chen J 2017 What is the main cause of grassland degradation? A case study of grassland ecosystem service in the middle-south Inner Mongolia *Catena* **150** 100–7
Williams C A, Collatz G J, Masek J and Goward S N 2012 Carbon consequences of forest disturbance and recovery across the conterminous United States *Glob. Biogeochem. Cycles* **26** GB1005
Yu J, Peng S and Chang J 2018 Inventory of methane emissions from livestock in China from 1980 to 2013 *Atmos. Environ.* **184** 69–76
Liu N, Kan H M and Yang G W 2015 Changes in plant, soil, and microbes in a typical steppe from simulated grazing: explaining potential change in soil C *Ecol. Monogr.* **85** 269–86
Vuichard N, Soussana J F O, Ciais P, Viovy N, Ammann C, Calanca P, Clifton-Brown J, Fuhrer J R, Jones M and Martin C 2007 Estimating the greenhouse gas fluxes of European grasslands with a process-based model: 1. Model evaluation from in situ measurements *Glob. Biogeochem. Cycles* **21** GB1004
No'am G S, Cavagnaro J B and HornoM E 1992 Simulation of defoliation effects on primary production of a warm-season, semiarid perennial-species grassland *Ecol. Model* **60** 45–61
Shiyomi M, Akiyama T,Wang S, Yiruhan A, Hori Y, Chen Z, Yasuda T, Kawamura K and Yamamura Y 2011 A grassland ecosystem model of the Xilingol steppe, InnerMongolia China *Ecol. Model* **222** 2073–83
Pan X, Guo X and Li X 2021 National Tibetan Plateau data center: promoting earth system science on the third pole *Bull. Amer. Meteor.* **102** E2062–78
Wang Z, Deng X and Song W 2017 What is the main cause of grassland degradation? A case study of grassland ecosystem service in the middle-south Inner Mongolia *Catena* **150** 100–7
FAOSTAT Online Statistical Service 2014 *Live animal numbers, crop production, total nitrogen fertiliser consumption statistics til 2014* (Food and Agriculture Organization (FAO)) (available at: http://faostat3.fao.org)
FAOSTAT Online Statistical Service 2018 *Live animal numbers, crop production, total nitrogen fertiliser consumption statistics til 2018* (Food and Agriculture Organization (FAO)) (available at: (https://doi.org/http://faostat3.fao.org))

IPCC 1997 Revised 1996 IPCC guidelines for national greenhouse gas inventories *Intergovernmental Panel on Climate Change*

Chang J, Peng S and Yin Y 2021 The key role of production efficiency changes in livestock methane emission mitigation *AGU Advances* **2** e2021AV000391

Change I C 2013 The physical science basis. Contribution of working group I to the fifth assessment report of the intergovernmental panel on climate change *IPCC Climate* **1535** 2013

Olivier J G J, Bouwman A F and Berdowski J J M 1996 *Description of EDGAR Version 2.0: A set of global emission inventories of greenhouse gases and ozone-depleting substances for all anthropogenic and most natural sources on a per country basis and on 1 degree x 1 degree grid* (Rijksinstituut voor Volksgezondheid en Milieu RIVM)